

# FAST-GSC: Fast and Adaptive Semantic Transmission for Generative Semantic Communication

Yiru Wang, Wanting Yang, Zehui Xiong, *Senior Member, IEEE*, Yuping Zhao, Shiwen Mao, *Fellow, IEEE*, Tony Q. S. Quek, *Fellow, IEEE*, H. Vincent Poor, *Life Fellow, IEEE*

**Abstract**—The rapidly evolving field of generative artificial intelligence technology has introduced innovative approaches for developing semantic communication (SemCom) frameworks, leading to the emergence of a new paradigm—generative SemCom (GSC). However, the complex processes involved in semantic extraction and generative inference may result in considerable latency in resource-constrained scenarios. To tackle these issues, we introduce a new GSC framework that involves fast and adaptive semantic transmission (FAST-GSC). This framework incorporates one innovative communication mechanism and two enhancement strategies at the transmitter and receiver, respectively. Aiming to reduce task latency, our communication mechanism enables fast semantic transmission by parallelizing the processes of semantic extraction at the transmitter and inference at the receiver. Preliminary evaluations indicate that while this mechanism effectively reduces task latency, it could potentially compromise task performance. To address this issue, we propose two additional methods for enhancement. First, at the transmitter, we employ reinforcement learning to discern the intrinsic temporal dependencies among the semantic units and design their extraction and transmission sequence accordingly. Second, at the receiver, we design a semantic difference calculation module and propose a sequential conditional denoising approach to alleviate the stringent immediacy requirement for the reception of semantic features. Extensive experiments demonstrate that our proposed architecture achieves a performance score comparable to the conventional GSC architecture while realizing a 52% reduction in residual task latency that extends beyond the fixed inference duration.

**Index Terms**—Semantic Communication, Generative AI, Prompt Engineering, Diffusion

## I. INTRODUCTION

THE imminent advent of sixth-generation (6G) networks is anticipated to experience an unparalleled increase in data traffic, fueled by the proliferation of cutting-edge applications such as ultra-high-definition video streaming, extended reality, and extensive Internet of Things (IoT) deployments. Concurrently, traditional communication systems are approaching their limit, and the scarcity of available spectrum resources

is becoming more pronounced. These factors collectively present substantial challenges in ensuring the quality of user experiences for these advanced services [1]. Recognizing the capacity of generative artificial intelligence (GAI) for modal transformation and its exceptional ability to produce high-quality content across various domains, generative semantic communication (GSC) presents a transformative solution. In GSC systems, task-related semantic information is distilled in the form of a *prompt*, which is transmitted to the receiver to guide the GAI models in inference [2]. This approach reduces the required data payload and enhances the overall efficiency of information exchange. Recent research validates the effectiveness of using image captions [3], segmentation maps [4], and skeleton maps [5] as prompts to reduce the transmission payload in image transmission scenarios.

However, owing to the elementary nature of the tasks addressed, the semantically homogeneous prompts employed in the referenced studies [3]–[5] fall short in scenarios characterized by complex demands and high-precision requirements. For example, in vehicular networks and the IoT, achieving comprehensive and precise inference at the user end necessitates the extraction and transmission of an extensive range of semantic data from the source [6], [7]. In vehicular networks, this includes data related to vehicle behavior, traffic conditions, and driver status, each representing distinct semantic categories that require precise processing to ensure both safety and efficiency. Similarly, in IoT environments, devices must interpret a diverse set of data inputs—from sensor outputs on machine performance to user interactions and environmental changes—enabling smarter home and industrial systems to dynamically adapt to variations in usage patterns, environmental conditions, and equipment status. The necessity to handle such a broad spectrum of data poses substantial challenges in resource-constrained environments. In these settings, distilling multi-type prompts requires sequential execution of various extraction models, which can significantly prolong the overall semantic extraction process. Meanwhile, in diffusion model-based GSC systems, achieving a high inference score necessitates iterative denoising procedures [8], which consequently induce considerable inference delays. The cumulative computation delays can potentially compromise the overall task completion speed and adversely affect the user experience.

In response to prevailing challenges, this work introduces a novel communication mechanism specifically engineered to reduce task latency. Contrary to traditional approaches that ne-

Yiru Wang is with Peking University, China, and also with Singapore University of Technology and Design, Singapore (yiruwang@stu.pku.edu.cn); Wanting Yang, Zehui Xiong and Tony Q. S. Quek are with the Pillar of Information Systems Technology and Design, Singapore University of Technology and Design, Singapore (e-mail: wanting\_yang@sutd.edu.sg; zehui\_xiong@sutd.edu.sg; tonyquek@sutd.edu.sg); Yuping Zhao is with Peking University, China (yuping.zhao@pku.edu.cn); Shiwen Mao is with the Department of Electrical and Computer Engineering, Auburn University, Auburn 36830, USA (e-mail: smao@ieee.org); H. V. Poor is with the Department of Electrical and Computer Engineering, Princeton University, Princeton, NJ 08544, USA (e-mail: poor@princeton.edu).

cessitate complete feature extraction prior to transmission, we sequentially and independently dispatch the extracted features to the receiver, facilitating fast semantic transmission. Building upon this fundamental mechanism, we refine both the prompt engineering approach at the transmitter and the diffusion-based inference approach at the receiver. These refinements enable us to tailor the semantic extraction sequence to precisely align with the task requirements and to enhance the overall guidance effectiveness of the sequentially transmitted semantic features on the task outputs, thereby fostering semantic adaptive transmission that is specifically attuned to the task goal. By synergistically integrating the proposed mechanism with these two approaches, we advance the development of a new GSC framework, termed FAST-GSC. This framework integrates fast and adaptive semantic transmission to concurrently reduce task latency while ensuring high task performance. The contributions of this work are outlined as follows:

- Initially, we introduce a novel communication mechanism within GSC systems, leading to the development of a fundamental framework, termed the Parallel Semantic Extraction and Inference-based GSC (PGSC) framework. This design significantly reduces task latency, particularly in complex scenarios that necessitate the extraction and transmission of multiple types of semantic features. Preliminary implementations of this framework suggest that the sequential dependencies among various units and the reception immediacy of individual units markedly influence system performance, highlighting the key directions for potential enhancement.
- On the transmitter side, we develop a novel prompt engineering approach that incorporates a temporal dimension to enhance task performance. Specifically, we employ a reinforcement learning (RL) model to discern the intrinsic sequential dependencies among the semantic units and adapt their extraction and transmission sequences according to the task. To simplify and accelerate the learning process, we implement the invalid action masking technique, which effectively excludes actions that do not contribute to the enhancement of the performance reward.
- On the receiver side, we introduce a sequential conditional denoising approach that adapts the diffusion-based inference process to the sequential transmission mechanism. Specifically, we devise a semantic difference calculation module that accurately identifies the areas within the noise space targeted by newly arrived semantic features. This identified difference is then applied to the predicted conditional noise, enhancing the guidance effectiveness of late-arriving semantic units and alleviating the stringent immediacy requirement for the reception of semantic features.
- In our experimental evaluation, we separately assess the effectiveness of the enhancements implemented at the transmitter and receiver sides. The efficacy of these enhancements is conclusively demonstrated through both quantitative analyses and visual evidence. Building upon this validation, we synergistically integrate these enhancements into the PGSC framework, culminating in the es-

tablishment of the FAST-GSC framework, which achieves a performance score comparable to the conventional GSC architecture while realizing a 52% reduction in residual latency that extends beyond the fixed inference duration.

The rest of this paper is organized as follows. In Section II, we review the related works. In Section III, we introduce the proposed PGSC framework and compare it with the conventional GSC design in respective of system latency. The motivations for refinement and the specific methods used to evolve the basic PGSC framework into the FAST-GSC framework are detailed in Section IV. The experimental evaluations are conducted in Section V, followed by the conclusions of the study and future works in Section VI.

## II. RELATED WORK

### A. Conditional Diffusion Models

Conditional diffusion models have emerged as a powerful class of generative models capable of producing high-quality samples across a range of data modalities. These models iteratively refine a distribution of noise to generate samples, conditioned on external information to guide the generation process towards desired characteristics. To exert a high degree of control over the generation process, a diverse array of conditions can be employed. Methods that leverage text for guidance have demonstrated remarkable capabilities across various media types [9], [10]. For delineating the contours of image objects, several studies have employed segmentation masks as conditioning inputs [11]. Additionally, the potential for manipulation through other modalities such as keypoints and depth maps has been explored, further expanding the versatility of control [12], [13].

Nonetheless, most current research introduces conditions at the start of the denoising process. Recently, [14]–[16] investigate the feasibility of collaborative distributed diffusion, aiming to reduce the total inference latency in multi-user scenarios by partitioning each user’s inference process into a co-denoising part executed at the edge device and a separate denoising part executed locally. However, because user-specific conditions are introduced midway through the denoising process, they may fail to effectively influence the inference results due to the already reduced noise levels. Therefore, each user’s inference performance may decrease compared to performing the entire denoising process independently. The issue of how to enhance the impact of temporally late-introduced conditions on inference results to improve overall inference performance remains an open question.

### B. Prompt Engineering

Recent research in this field indicates that advanced models like DALL-E [17], Stable Diffusion [18], and GPT-4 [19] respond variably to subtle nuances in language, where even minor modifications in the prompt can lead to significantly different outputs. In light of this phenomenon, prompt engineering emerges as a crucial technique for boosting the performance of GAI models. Within this field, several methods are prominently utilized. For example, keyword-based prompting

is a prompt engineering approach that incorporates specific keywords or phrases to guide the model's attention, ensuring alignment with the desired topic or context [20]. Context-rich prompting provides detailed scenarios or background information to frame the response accurately, making the generated output more contextually appropriate and relevant [21], [22]. Iterative refinement adjusts prompts based on feedback and results, allowing for continuous improvement in the model's performance [23].

Nonetheless, given that the temporally segmented denoising approach has only recently been introduced in references [14]–[16], the implementation of prompt engineering in a time-sequential manner remains areas yet to be explored.

### C. Model Acceleration

As deep learning models become more complex, their high computational demands can limit practical applications, particularly on resource-constrained devices. To address this, integrating latency considerations directly into the architecture search process has emerged as an effective solution. This approach facilitates the development of models that are intrinsically optimized for enhanced performance on specific hardware configurations [24]. Additionally, model compression techniques such as pruning and quantization are increasingly recognized for their ability to reduce model size and computational complexity, thereby decreasing latency [25]. Knowledge distillation represents another promising strategy, where a compact, efficient model is trained to mimic the behavior of a larger, more intricate model [26].

Instead of solely focusing on individual models, we aim to propose to reduce the overall task latency from a holistic system perspective. Additionally, integrating the methodology developed in this study with the aforementioned model optimization techniques could further diminish system delays.

## III. PGSC: FRAMEWORK AND KEY COMPONENTS

In this work, we concentrate on image transmission scenarios due to their widespread prevalence and demonstrative nature. However, it is essential to note that our approach is also applicable to a variety of transmission scenarios and different data modalities. Herein, the receiver is an image renderer that produces images of varying levels of detail based on different task requirements. The transmitter, on the other hand, is an end device with limited computational capabilities and resources, responsible for capturing the key features of the source images according to the receiver's request.

The PGSC framework can be divided into distinct modular functional components, including semantic extraction, wireless transmission, and diffusion-based inference. In the following, we first introduce semantic extraction and diffusion-based inference processes. Next, we compare the proposed PGSC framework with conventional GSC frameworks in terms of system latency and communication mechanisms.

### A. Semantic Extraction

Similar to GSC, the extraction process is dedicated to deriving semantic representations from the original source

data. While existing extraction models, such as specific image captioning algorithms, are capable of distilling summary-level information from images through a single operation, they frequently generate prompts that are overly generalized and deficient in detailed specificity [27], [28]. Consequently, they may not be suitable in scenarios with high precision demands. Therefore, we deploy a series of extraction models at the transmitter, each specifically designed to accurately extract a certain type of semantic description by leveraging its specialized knowledge. The activation of these models depends on the task requests received from the receiver. Herein, we denote each extraction result as a *semantic unit*, and refer to the collection of all semantic units from an image as a *prompt*.

We denote the source image as  $\mathbf{s} \in \mathbb{R}^{c \times h \times w}$ . The semantic extraction process of distilling the  $k$ th semantic unit  $\mathbf{u}_k$  can be expressed by

$$\mathbf{u}_k = f_k(\mathbf{s}; \boldsymbol{\psi}_k), \quad (1)$$

where  $\boldsymbol{\psi}_k$  represents the trainable parameters of the extraction model for distilling  $\mathbf{u}_k$ ,  $K$  represents the maximum number of semantic units and  $\forall k \in \{0, 1, \dots, K-1\}$ .

### B. Diffusion-based Inference

Inspired by the significant success of diffusion models across a wide range of real-world generative inference tasks, the Stable Diffusion model [18] is commonly employed for generative inference at the receiver within the GSC framework [2], [3]. Its goal is to generate images that semantically adhere to the provided prompt.

The stable diffusion model is built upon the denoising diffusion probabilistic model (DDPM) [8], which is capable of learning a distribution  $p_\theta(\mathbf{x}_0)$  that approximates  $q(\mathbf{x}_0)$ . It can be treated as a latent variable model of the form  $p_\theta(\mathbf{x}_0) = \int p_\theta(\mathbf{x}_{0:T}) d\mathbf{x}_{1:T}$ , where  $\mathbf{x}_1, \dots, \mathbf{x}_T$  are called latents of the same dimensionality as the original data  $\mathbf{x}_0 \sim q(\mathbf{x}_0)$ . The joint distribution  $p_\theta(\mathbf{x}_{0:T})$  is called the *reverse process*, which can be formulated as  $p_\theta(\mathbf{x}_{0:T}) = p(\mathbf{x}_T) \prod_{t=1}^T p_\theta(\mathbf{x}_{t-1} | \mathbf{x}_t)$ .

The learning process starts from a pure noise image  $\mathbf{x}_T \sim \mathcal{N}(\mathbf{x}_T; \mathbf{0}, \mathbf{I})$ . The Markov chain with learned Gaussian transition can be expressed by  $p_\theta(\mathbf{x}_{t-1} | \mathbf{x}_t) = \mathcal{N}(\mathbf{x}_{t-1}; \mu_\theta(\mathbf{x}_t, t), \boldsymbol{\Sigma}_\theta(\mathbf{x}_t, t))$ . To facilitate the learning process, a *forward process* or *diffusion process*  $q(\mathbf{x}_{1:T} | \mathbf{x}_0) = \prod_{t=1}^T q(\mathbf{x}_t | \mathbf{x}_{t-1})$  is implemented, which is a fixed Markov chain that gradually adds Gaussian noise to the data according to a variance schedule  $\beta_1, \dots, \beta_T$ , as  $q(\mathbf{x}_t | \mathbf{x}_{t-1}) = \mathcal{N}(\mathbf{x}_t; \sqrt{1 - \beta_t} \mathbf{x}_{t-1}, \beta_t \mathbf{I})$ . Denote  $\alpha_t = 1 - \beta_t$  and  $\bar{\alpha}_t = \prod_{s=1}^t \alpha_s$ , we can sample  $\mathbf{x}_t$  at timestep  $t$  as  $q(\mathbf{x}_t | \mathbf{x}_0) = \mathcal{N}(\mathbf{x}_t; \sqrt{\bar{\alpha}_t} \mathbf{x}_0, (1 - \bar{\alpha}_t) \mathbf{I})$ . Subsequently, the forward posteriors conditioned on  $\mathbf{x}_0$  can be expressed by

$$q(\mathbf{x}_{t-1} | \mathbf{x}_t, \mathbf{x}_0) = \mathcal{N}(\mathbf{x}_{t-1}; \tilde{\mu}_t(\mathbf{x}_t, \mathbf{x}_0), \tilde{\beta}_t \mathbf{I}), \quad (2)$$

where  $\tilde{\mu}_t(\mathbf{x}_t, \mathbf{x}_0) = \frac{\sqrt{\bar{\alpha}_{t-1} \beta_t}}{1 - \bar{\alpha}_t} \mathbf{x}_0 + \frac{\sqrt{\bar{\alpha}_t (1 - \bar{\alpha}_{t-1})}}{1 - \bar{\alpha}_t} \mathbf{x}_t$  and  $\tilde{\beta}_t = \frac{1 - \bar{\alpha}_{t-1} \beta_t}{1 - \bar{\alpha}_t} \beta_t$ . The target of the learning process of DDPM is to minimize the gap between  $q(\mathbf{x}_{t-1} | \mathbf{x}_t, \mathbf{x}_0)$  and  $p_\theta(\mathbf{x}_{t-1} | \mathbf{x}_t)$ .

When the coefficient of variance is considered as a constant, this goal is equivalent to predicting  $\mu_\theta(\mathbf{x}_t, t)$  that as accurately as possible to match  $\tilde{\mu}_t(\mathbf{x}_t, \mathbf{x}_0)$ . Denote  $\mathbf{y}$  as the prompt, the loss function during training is formulated as the difference between the generated noise  $\varepsilon$  and predicted noise  $\varepsilon_\theta(\mathbf{x}_0, t, \mathbf{y})$ , as follows [18]:

$$\mathcal{L} = \mathbb{E}_{t, \mathbf{y}, \mathbf{x}_t, \varepsilon} \left[ \left\| \varepsilon - \varepsilon_\theta \left( \sqrt{\alpha_t} \mathbf{x}_0 + \sqrt{1 - \alpha_t} \varepsilon, t, \mathbf{y} \right) \right\|_2^2 \right]. \quad (3)$$

During sampling, the noise estimation can be performed by classifier-free guidance [29], which is expressed by

$$\tilde{\varepsilon}_\theta(\mathbf{x}_t, \mathbf{y}, t) = \varepsilon_\theta(\mathbf{x}_t, \mathbf{y}, t) + w \cdot (\varepsilon_\theta(\mathbf{x}_t, \mathbf{y}, t) - \varepsilon_\theta(\mathbf{x}_t, t)), \quad (4)$$

where  $w$  is the guidance scale.

As DDPM necessitates executing all consecutive denoising steps to produce the clean sample  $\mathbf{x}_0$ , it results in significant task latency. In light of this, we adopt the sampling method of the denoising diffusion implicit model (DDIM) [30], which allows for skipping some denoising steps without compromising the quality of the inferred images. This method enhances DDPM by leveraging a non-Markovian inference process, which can be formulated as

$$\mathbf{x}_{t-1} = \sqrt{\alpha_{t-1}} \left( \frac{\mathbf{x}_t - \sqrt{1 - \alpha_t} \tilde{\varepsilon}_\theta(\mathbf{x}_t, \mathbf{y}, t)}{\sqrt{\alpha_t}} \right) + \sqrt{1 - \alpha_{t-1}} \cdot \tilde{\varepsilon}_\theta(\mathbf{x}_t, \mathbf{y}, t). \quad (5)$$

### C. Latency Discussion and Communication Mechanism

The task latency can be categorized into the following three components:

1) *Semantic Extraction Latency*: Due to limited computational resources, the extraction process proceeds sequentially. Consequently, the aggregate latency of the entire extraction procedure can be expressed as

$$\tau_{ext} = \sum_{k=0}^{K-1} \tau_k, \quad (6)$$

where  $\tau_k$  is the latency for extracting the  $k$ th semantic unit. In practice,  $\tau_k$  hinges on the efficiency of each extraction model and the computational power available at the transmitter, with durations extending from milliseconds to seconds [31]–[33].

2) *Diffusion-based Inference Latency*: In the inference process, the latency is determined by the total number of denoising steps  $M$ , which can be formulated as

$$\tau_{gen} = \sum_{m=0}^{M-1} \tau_m, \quad (7)$$

where  $\tau_m$  is the inference latency of the denoising step  $m$  and  $m \in \{0, 1, \dots, M-1\}$ . In practice,  $\tau_m$  depends on the computational resources of the receiver, varying from milliseconds to seconds [34], [35].

3) *Wireless Transmission Latency*: Generally, the prompts distilled in GSC systems are concise and highly compressed [2], [3]. Consequently, leveraging the capabilities of 5G technology can significantly reduce the transmission latency,  $\tau_{trans}$ , to less than one millisecond [36].

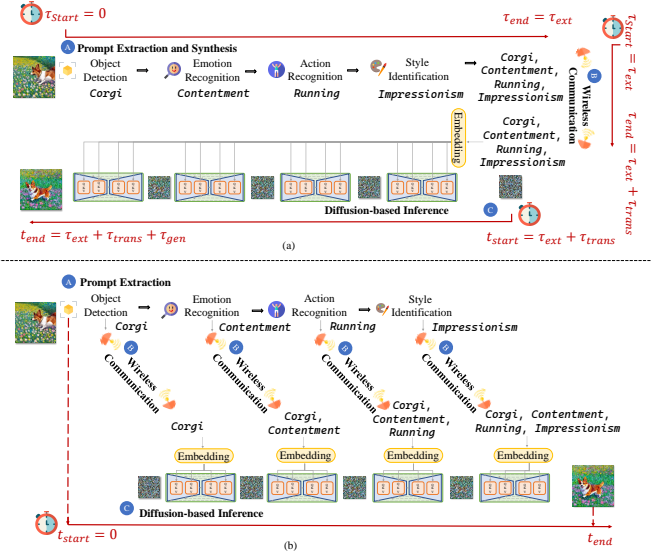


Fig. 1. Comparison of communication mechanisms and system latency. (a) Conventional GSC framework, where transmission starts after the completion of all semantic extraction; (b) Proposed PGSC framework, where semantic extraction and diffusion-based inference are executed in parallel.

Based on the investigations above, it is evident that the latencies associated with extraction and inference significantly exceed those of transmission. Therefore, the system latency is primarily influenced by the extraction and inference processes. Under complex requirements, extensive semantic unit extraction is essential to thoroughly capture the semantic attributes of the source. Concurrently, executing a high number of denoising steps is crucial to ensure the precision of inference results. Consequently, the combination of these procedures leads to significant system latency.

In conventional GSC, the aforementioned processes operate in a temporally disjointed manner, resulting in cumulative latency. By contrast, in PGSC, we propose executing the semantic extraction and diffusion-based inference in parallel. Specifically, the diffusion model's denoising process is initiated by the first received semantic units. In subsequent stages, newly arrived semantic units combine with previously arrived units to collectively guide the denoising process. A comparison of the communication mechanisms and system latency of the conventional GSC and our PGSC is presented in Fig. 1.

## IV. FROM PGSC TO FAST-GSC: MOTIVATIONS AND APPROACHES

In this section, we commence by outlining our refinement motivations, which are based on our examination of the PGSC framework's implementation. Subsequently, we elucidate our enhancements from the perspectives of both the transmitter and the receiver.

### A. Refinement Motivations

Although the PGSC framework allows for continuous conditioning on received semantic units, thereby reducing system latency resulting from the prolonged extraction process, this approach can potentially lead to significant task performance

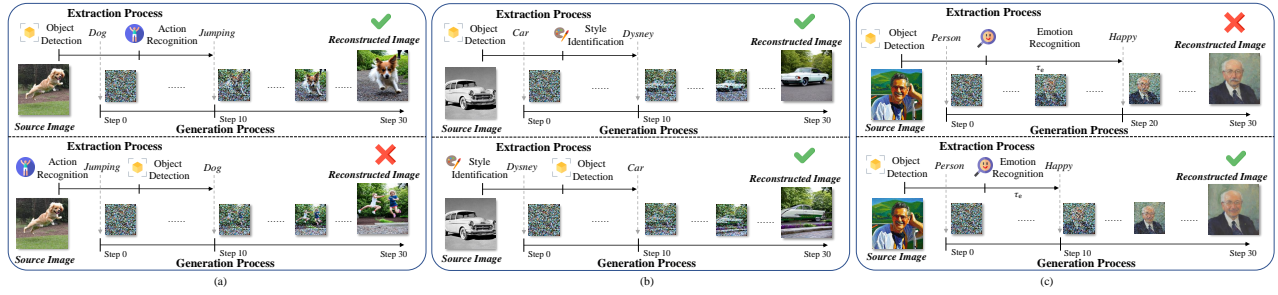


Fig. 2. Illustrative examples of some direct implementations of the PGSC framework. The total denoising step is set at 30 for all schemes. In (a), the switch of the execution order of these two extraction models yields semantically different results. In (b), the switch of the execution order of the two extraction models doesn't change the semantic meanings of inference results. In (c), we posit that the speed of the emotion recognition model on the upper side is slower than on the lower side, leading to the emotion-related semantic unit on the upper side arriving 10 steps later than on the lower side. Observations indicate that the inferred image on the lower side effectively incorporates guidance from both extracted semantic units, whereas the upper one fails to integrate the second semantic feature.

loss. To better illustrate, we present three representative examples illustrated in Fig. 2 and summarize two key factors determining the task performance of PGSC as follows:

1) *Sequential Dependencies Among Various Units*: Given that different semantic units influence varying aspects and extents of the inference results, they also exhibit diverse degrees of sequential dependencies during the inference process. As illustrated in Fig. 2 (a), with the same extraction speed, changing the extraction and transmission sequence between two semantic units can yield significantly different outcomes. This phenomenon demonstrates the tight sequential dependency between these two semantic units during the inference process of the diffusion model. In contrast, as shown in Fig. 2 (b), switching the extraction and transmission sequence between another pair of semantic units results in similar inference outcomes both semantically and visually, indicating a weak sequential dependency between these units.

2) *Reception Immediacy of Individual Units*: In the PGSC framework, the denoising process begins after the reception of the first semantic unit. As the denoising process progresses, the noise level diminishes, limiting the capacity to incorporate new semantic features. As depicted in the upper part of Fig. 2 (c), due to the excessive processing delays of the second extraction model, the receiver can only integrate the second semantic unit into the conditional guidance at the 20th denoising step. The minimal remaining noise at the 20th denoising step limits the modification capacity of the second semantic unit, resulting in a certain degree of semantic mismatch between the source and inferred images. If the reception timestamp of the second semantic unit is 10 denoising steps earlier, its influence can still be observed, as shown in the lower part of Fig. 2 (c).

In light of these analyses, we propose enhancing the system performance of the PGSC framework from two perspectives: 1) From the transmitter's perspective, we aim to learn the intrinsic sequential dependencies among various semantic units and strategically design their extraction and transmission order accordingly; and 2) From the receiver's perspective, we aim to mitigate the stringent reception immediacy and enhance the guidance effectiveness of the late-arrived semantic units for the final performance. The details of these two approaches are presented in the following content.

### B. Perspective from Transmitter: Temporal Prompt Engineering

At the transmitter, our goal is to guide the diffusion model to produce the desired output by regulating the input. This is akin to the objective of prompt engineering [22], except that we need to achieve this from a temporal perspective, forming a temporal prompt engineering approach. Given our observation that the order of extraction and transmission of different semantic units should follow their sequential dependencies, we resort to RL to learn and implement this strategy. Its aim is to ensure the final inferred images bear a close resemblance to the comprehensive prompt, while simultaneously minimizing system latency as much as possible. The designs of the fundamental components are outlined in the following content.

1) *MDP Constructing*: In constructing the RL model, we frame the interaction between the agent and the environment as a Markov Decision Process (MDP). The MDP can be defined as a three-component tuple  $(\mathcal{S}, \mathcal{A}, r)$ , where  $\mathcal{S}$  is state space set,  $\mathcal{A}$  is the action space set, and  $r$  is the reward function. Within this framework, an episode is defined as a complete trajectory from the initial state to the terminal state, consisting of a sequence of states, actions, and corresponding rewards. To simplify the learning process of RL models, we divide the inference process into multiple segments at equal intervals. At the beginning of each inference segment, only newly arrived semantic units can be integrated with previously arrived ones to guide the denoising. This approach allows the RL model to learn reception deadlines of semantic units with different attributes, thereby establishing the extraction and transmission sequence. To better illustrate the MDP in our study, we depict an episode in Fig. 3 and the detailed design of this framework is given as follows:

**State**: We include the task-related request in the agent's state, which contains the attribute and quantity of semantic units required by the receiver. To facilitate the learning of the RL model, we can employ one-hot encoding to preprocess the semantic attributes. Let  $e_{k,t}$  denote the encoded  $N_e$ -length one-hot vector for the  $k$ -th required semantic attribute at phase<sup>1</sup>  $t$ , where the  $n_e$ -th position is set to 1, corresponding

<sup>1</sup>In our work, the term 'phase' corresponds to a single iteration or transition within the RL environment, with each phase forming a segment of an episode.



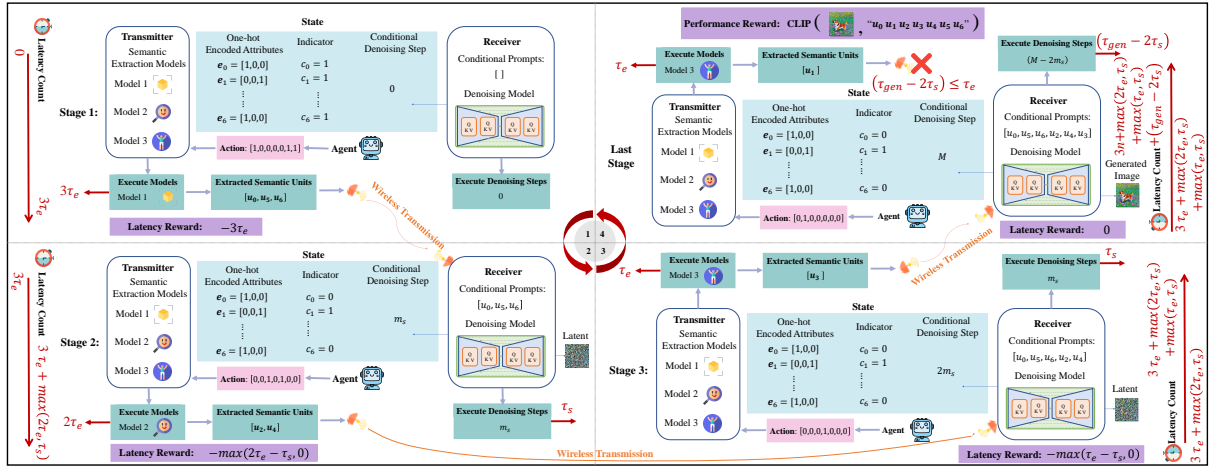


Fig. 3. Illustration depicting an example of a single episode within the MDP framework. In the first RL phase, all indicators are set to one, and the agent selects the extraction model to be executed at this phase. As the denoising process has not yet started, these semantic units can be integrated into the diffusion model from the initial denoising step. At the beginning of the second RL phase, the extracted results distilled at the first RL phase arrive at the receiver and initiate the denoising process. The indicators corresponding to the transmitted units are set to zero. In the final phase, the denoising process reaches its scheduled total phase and terminates the episode. Given that the extraction latency surpasses the denoising duration at this phase, one semantic unit remains unsuccessfully transmitted.

to the activation of the  $n_e$ -th extraction model to obtain the relevant semantic unit. When the requested number of semantic units is less than  $K$ , we fill the remaining positions in the one-hot encoding with zero vectors. Subsequently, the entire encoded one-hot matrix for the whole prompt can be expressed by  $\mathbf{E}_t = [e_{0,t}, \dots, e_{K-1,t}]$ . Since the residual noise levels vary at different denoising steps, and the allowable space for modifications also changes, the decision-making process of the RL model should include the conditional denoising step of the diffusion model  $d_t$  as part of its state, which indicates the starting denoising step from which the semantic units selected at time  $t$  can guide. When  $d_t$  reaches the designated maximum number of denoising steps, it signifies the conclusion of the episode. To distinguish whether the semantic units are still required by the receiver at phase  $t$ , we also design a binary  $K$ -length vector  $\mathbf{c}_t$  as an indicator. When an element of this vector is set to 0, it indicates that the corresponding semantic unit has either been transmitted or the associated one-hot attribute vector is a zero vector. The element is set to 1 otherwise. Therefore, the corresponding state observed by the agent at time phase  $t$  is denoted as  $\mathbf{s}_t = [\mathbf{E}_t, \mathbf{c}_t, d_t]$ .

**Action:** The action executed by the agent at time  $t$  is denoted by  $\mathbf{a}_t = [a_0, \dots, a_{K-1}]$ , where  $a_k \in \{0, 1\}$  for  $k = 0, \dots, K - 1$ . The practical implication of this action is that, when the agent selects certain semantic attributes, the corresponding extraction models that distill the semantic units with the selected attributes are executed at this RL phase.

**Reward:** Aligned with our objectives of ensuring high inference precision while reducing task latency, the reward is a composite of two components: the system's *performance reward* and the *latency reward*. Similar to [2], we adopt the CLIP score [37] as the performance reward in our work. This metric assesses the semantic similarity between the inferred images and the corresponding prompts within the embedding

space of CLIP model [38], which can be expressed by

$$r_p = \text{CLIP-S} = w_1 \cdot \max(\cos(\mathbf{h}, \mathbf{v}), 0), \quad (8)$$

where  $\mathbf{h}$  represents the prompt's embedding,  $\mathbf{v}$  denotes visual embedding and  $w_1 = 1$  in our work. Given that the intermediate results in the denoising process are inherently noisy [8], [18], [30], they can not directly reflect the semantics and qualities of the final images. Consequently, the reward is calculated and assigned to the agent only after the completion of the entire denoising process<sup>2</sup>.

Building on the PGSC framework, system latency is determined by the degree of parallel execution between semantic extraction and inference processes. Specifically, in the first phase of each episode, the receiver has not yet received any semantic units, and thus, denoising has not yet started. The latency of this phase is entirely determined by the execution time of the selected extraction model. From the second phase onward, the receiver can condition on the received semantic units, and extraction at the transmitter and inference at the receiver start simultaneously. The latency of these phases is determined by the maximum latency of either the transmitter's semantic extraction or the receiver's segmented denoising. Thus, instead of calculating system latency at the conclusion of one episode, we can expedite the learning process by defining the latency reward as the additional extraction delay relative to the segmented denoising duration at each phase. Therefore, the combined reward obtained at phase  $t$  can be formulated as

$$r_t = \begin{cases} -\tau_e \cdot n_t & t = 0, \\ -\max((\tau_e \cdot n_t - \tau_s), 0) & 1 \leq t < L - 1, \\ -\max(\mathbf{1}_{nor} \cdot (\tau_e \cdot n_t - \tau_s), 0) + r_p & t = L - 1, \end{cases} \quad (9)$$

<sup>2</sup>Should an efficient and rapid methodology for assessing semantics from partially denoised images be established, it would enable the deployment of some reward shaping techniques [39], [40] for addressing this sparse reward and accelerating the training of the RL model. This area of research remains open for future studies.

where  $\tau_e$  denotes the latency for extracting a single semantic unit,  $n_t$  denotes the number of selected semantic units at RL phase  $t$ ,  $\tau_s$  is time delay for executing the segmented denoising steps.  $L$  denotes the number of phases in one episode, which varies with each episode. Its value depends on the number of semantic units required for transmission in each round and the progress of model learning. The index factor,  $\mathbf{1}_{nor}$ , equals 1 if the distilled semantic units at this phase can be received before the conclusion of the denoising process, and 0 otherwise.

Finally, the long-term reward for the agent can be calculated as the sum of the discounted rewards obtained at each phase in an episode, which is expressed by

$$r = \sum_{t=0}^{L-1} \gamma^t \cdot r_t, \quad (10)$$

where  $\gamma$  is a discount factor.

2) *Learning Principle*: Building on the MDP framework described above, we propose utilizing the Proximal Policy Optimization (PPO) [41] algorithm to identify the optimal strategy for dispatching semantic units. PPO is a policy gradient method that directly updates a stochastic policy neural network,  $\pi_\varphi$ , to model the action distribution for a given state as  $\pi_\varphi(\mathbf{s}, \mathbf{a})$ . Generally, the PPO algorithm employs three neural networks: the current policy network  $\pi_\varphi$  with parameter  $\varphi$ , the last updated policy network  $\pi_{\varphi'}$  with parameter  $\varphi'$  and a critic network  $V_\phi$  with parameter  $\phi$ . Both the new and old policy networks generate the action's probability distribution under the current state, with the old policy network serving to constrain the variance of the new policy. The critic network estimates the state value function for the current state, which assesses the performance of the new policy network.

To efficiently leverage experiences gathered under an old policy  $\pi_{\varphi'}(\mathbf{a}_t | \mathbf{s}_t)$  for estimating potential performance under a new policy  $\pi_\varphi(\mathbf{a}_t | \mathbf{s}_t)$ , we can define the probability ratio between the new policy and the old policy as  $r_t(\varphi) = \frac{\pi_\varphi(\mathbf{a}_t | \mathbf{s}_t)}{\pi_{\varphi'}(\mathbf{a}_t | \mathbf{s}_t)}$ . Subsequently, the clipped surrogate objective in PPO algorithm is formulated by

$$\mathcal{L}_t^{\text{clip}}(\varphi) = \hat{\mathbb{E}}_t \left[ \min(r_t(\varphi)\hat{A}_t, \text{clip}(r_t(\varphi), 1 - \eta, 1 + \eta)\hat{A}_t) \right], \quad (11)$$

where  $\text{clip}(\cdot)$  is the clip function which prevents the new policy from going far away from the old policy by limiting the probability ratio to the interval  $[1 - \eta, 1 + \eta]$ .  $\hat{A}_t$  represents the estimated advantage function, given by  $\hat{A}_t = \delta_t + (\gamma\lambda)\delta_{t+1} + \dots + (\gamma\lambda)^{T-t+1}\delta_{T-1}$ , where  $\gamma$  is the discount factor and  $\lambda$  is the trace-decay parameter.  $\delta_t = r_t + \gamma V_\phi(\mathbf{s}_{t+1}) - V_\phi(\mathbf{s}_t)$  represents the temporal difference error, and  $V_\phi(\mathbf{s}_t)$  is the state value function output by the critic network with parameter  $\phi$ . The critic network is updated by gradient descent, i.e.  $\phi = \phi - \alpha \nabla_\phi \mathcal{L}(\phi)$ , where  $\mathcal{L}(\phi)$  is the loss function for the critic network, which is a mean squared error function defined as  $\mathcal{L}(\phi) = \mathbb{E} \left[ \left( \sum_{\tau=0}^{\infty} \gamma^\tau r_{t+1+\tau} - V_\phi(\mathbf{s}_t) \right)^2 \right]$ .

Moreover, to encourage exploration and prevent the agent from falling into a suboptimal situation, we incorporate the entropy of the probability distribution into the loss function to

increase the policy's exploration of actions. Finally, the loss function for the new policy network can be expressed by

$$\mathcal{L}_t^{\text{PPO}}(\varphi) = \mathcal{L}_t^{\text{clip}}(\varphi) + \xi \cdot S_{\pi_\varphi}(\mathbf{s}_t), \quad (12)$$

where  $S_{\pi_\varphi}(\mathbf{s}_t)$  is the entropy of the new policy network at time phase  $t$  and  $\xi$  denotes the entropy coefficient.

3) *Invalid Action Masking*: In complex task scenarios, the receiver may require a substantial number of semantic units. Our action space, which expands exponentially with the maximum required number of semantic units for transmission, can significantly impede the learning process. To streamline this, we propose excluding certain actions at each RL phase that fail to provide valuable semantic information to the receiver. These actions do not contribute to the integration of new semantic attributes into the inferred images, thereby not enhancing the performance score. Furthermore, these actions also squander transmission resources that could be more effectively allocated to conveying other informative semantic units within the specified transmission deadlines. In our work, we identify two types of non-contributory actions: 1) Actions intended to distill semantic units associated with a zero-vector in their one-hot attribute representation; and 2) Actions aimed at distilling semantic units that have already been extracted and transmitted. By removing these non-contributory actions from the action space, we can simplify and accelerate the learning process of the RL model. The effectiveness of this approach is validated through simulations, as detailed in Section V-A.

To achieve this, we utilize the invalid action masking technique [42], which is commonly implemented to avoid repeatedly generating invalid actions in large discrete action spaces. Specifically, we set the logits associated with the aforementioned non-contributory actions to  $-\infty$  and normalize the probabilities of all the actions by

$$\text{softmax}(z_i) = \frac{e^{z_i}}{\sum_{j=0}^{N_A} e^{z_j}}, \quad (13)$$

where  $z_i$  is the model's output probability distribution of action  $\mathbf{a}_i$ .  $N_A$  denotes the total number of actions in the action set, which equals to  $2^K$  in our work. The probability of sampling invalid actions is equal to 0 as  $\lim_{z \rightarrow -\infty} e^z = 0$ .

### C. Perspective from Receiver: Sequential Conditional Denoising

At the receiver, we aim to mitigate the stringent reception immediacy, thereby enabling the sequentially arrived units to continuously contribute to the inference results. To achieve this goal, one straightforward method is to add a certain amount of noise to the inference process every time a new semantic unit arrives at the receiver, ensuring enough space for modifications. However, this approach increases the overall noise level, requiring additional denoising steps and significantly prolonging the inference process.

Inspired by the classifier-free guidance [29], we propose a sequential conditioning denoising approach to enhance the intervention capability of late-arrived semantic units for final performance without disrupting the ongoing denoising

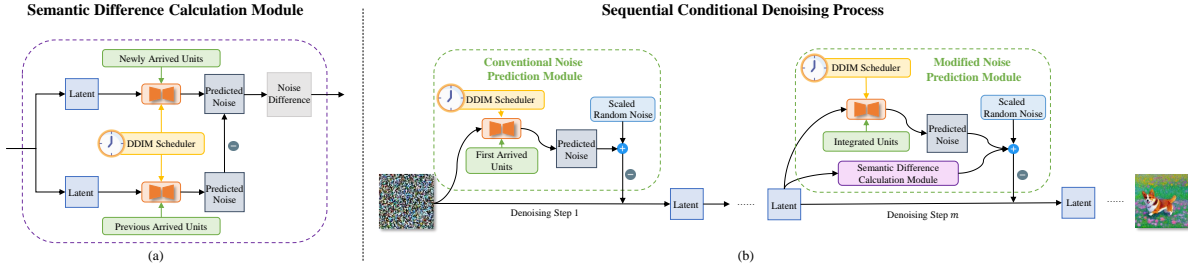


Fig. 4. Demonstration of the refinements at the receiver. (a) Workflow of the proposed semantic difference calculation module; (b) Illustration of the sequential conditional denoising process, where the guidance effectiveness of late-arrived semantic units is enhanced for improved final performance.

schedule. Specifically, we first introduce a semantic difference calculation module that can output the difference between the estimated conditional noises guided by the newly received and the previously received semantic features, as depicted in Fig. 4 (a). Contrary to blindly introducing random noise to all the intermediate results, this module allows us to precisely and efficiently identify the space the newly arrived semantic features target to modify at the current denoising step. Subsequently, we supplement the noise difference to the estimated noise conditioned on all the received semantic features using a weighted sum method. Building upon Equation (4), this modification can be formulated as follows:

$$\begin{aligned} \hat{\epsilon}_\theta(\mathbf{x}_t, \mathbf{y}_{\text{combined}}, \mathbf{y}_{\text{new}}, \mathbf{y}_{\text{previous}}, t) &= \tilde{\epsilon}_\theta(\mathbf{x}_t, \mathbf{y}_{\text{combined}}, t) \\ &+ \alpha \cdot (\epsilon_\theta(\mathbf{x}_t, \mathbf{y}_{\text{new}}, t) - \epsilon_\theta(\mathbf{x}_t, \mathbf{y}_{\text{previous}}, t)), \end{aligned} \quad (14)$$

where  $\alpha$  is the intervention factor,  $\mathbf{y}_{\text{combined}}$  denotes all the semantic units received at diffusion step  $t$ ,  $\mathbf{y}_{\text{new}}$  denotes the semantic units newly received at diffusion step  $t$  and  $\mathbf{y}_{\text{previous}}$  denotes the semantic units received before diffusion step  $t$ . Through this approach, the guidance effectiveness of late-arrived semantic units for final performance can be enhanced, which can mitigate the issue of many semantic features not being effectively incorporated into the inference results due to their late extraction and transmission in complex tasks. The overall sequential conditional denoising process is illustrated in Fig. 4 (b).

## V. PERFORMANCE EVALUATION

In this section, we implement the proposed PGSC framework, as well as the two refinement approaches. We conduct extensive experiments that target to answer the following three questions: 1) whether the designed temporal prompt engineering approach can capture the intrinsic sequential dependencies among various semantic units, thereby optimizing the extraction and transmission order to enhance inference performance; and 2) whether the proposed sequential conditional denoising approach can improve the guidance effectiveness of late-arriving semantic units for final performance, thereby mitigating the strict reception immediacy constraints; and 3) whether the two approaches can work synergistically to reduce overall latency while ensuring high task performance. The details of implementations and the analysis of the experimental results are also described.

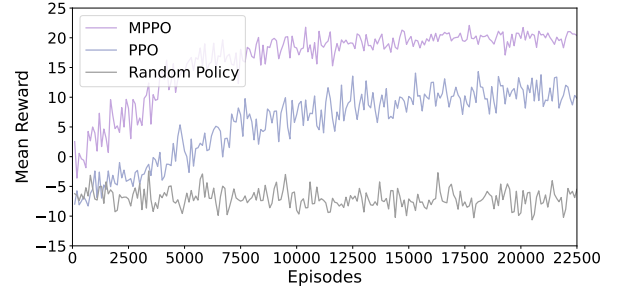


Fig. 5. Learning performance of MPPO, PPO and random policy.

**Datasets:** We utilize the text sentences from the DIFFUSIONDB [43] dataset as extracted prompts for both training and testing purposes. This dataset stands as the first extensive text-to-image prompt repository, exhibiting a wide array of syntactic and semantic attributes. We limit the length of the prompts to between 6 and 12 words, which reduces the dataset to approximately 0.2 million usable prompts. This dataset is divided into training and testing sets following a 9:1 ratio. We categorize each text word’s semantic attribute into five types: NOUN, ADJECTIVE, STYLE<sup>3</sup>, VERB, and OTHERS. Subsequently, we employ spaCy [45] to segment the prompts into semantic units and tag each unit correspondingly [46].

**Experimental Settings:** We employ Stable Diffusion v1-4<sup>4</sup> as the generative inference model at the receiver and base our optimization strategies on it. As analyzed in Section III-C, the wireless transmission delay is negligible for text prompt transmission. Therefore, we exclude this delay from our experiments. The experiments are conducted on a server with an NVIDIA RTX 4090 GPU with 24 GB of memory. The operating system is Ubuntu 20.04 with Pytorch 2.0.1.

**Hyperparameters:** We set the total number of denoising steps  $M$  at 60. By default, we segment the entire process into intervals of 10 denoising steps and equate the extraction latency of distilling one text unit from the source image to 5 denoising steps. The learning rate is established at 0.009. The entropy coefficient  $\xi$  is set at 0.01, the discount factor  $\gamma$  is set at 0.99 and the  $\eta$  parameter in the clip function is fixed at 0.2.

<sup>3</sup>In our work, the style-related text words include 51 types of styles as detailed in [44], along with words that have proper noun properties.

<sup>4</sup><https://huggingface.co/CompVis/stable-diffusion-v1-4>



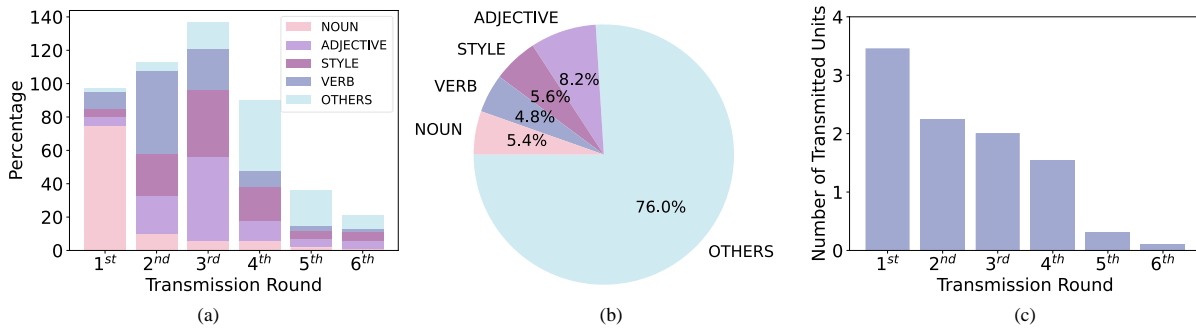


Fig. 6. Statistical results of the TPE method. (a) Semantic characteristics of text units transmitted in chronological order; (b) Composition of discarded text units; (c) Number of text units transmitted in chronological order. According to our statistical results, six represents the maximum transmission round, as the number of text units transmitted from the seventh transmission onward is zero.

### A. Effectiveness of Temporal Prompt Engineering

In this part, we evaluate the effectiveness of the proposed temporal prompt engineering (TPE) method. Initially, we demonstrate the training process of our invalid action masking-assisted PPO model and compare its performance with that of two traditional methods. Subsequently, we conduct the statistical analysis of the trained model’s results and investigate the presence of semantic patterns in its decision-making process.

1) *Training Process*: The learning curves of the agents under different settings are shown in Fig. 5. We compare our invalid action masking-assisted PPO method (MPPO) against the conventional PPO method without masking and the random policy. It can be observed that our proposed MPPO algorithm offers notable enhancements compared to the one without masking in both convergence speed and the final values achieved. This superior performance can be attributed to the use of invalid action masking, which assists in eliminating non-contributory actions. This approach ensures that different semantic units are continually incorporated throughout the limited denoising process, enriching the content of the final inferred image and enhancing image quality. Additionally, as the number of transmissions increases, an increasing number of actions are identified and masked as non-contributory, leading to a faster learning speed and improved convergence of the algorithm.

2) *Statistic Analysis*: Subsequently, we analyze the statistical results of the TPE method. First, we explore the semantic characteristics of text units sent in chronological order, as illustrated in Fig. 6 (a)<sup>5</sup>. These results reveal that the TPE method preferentially initiates the transmission of nouns. Consequently, extraction models that target noun retrieval, such as those used for object and scene recognition, should be prioritized in execution. During the second round of transmission, action-related units are more likely to be selected, corresponding to the outputs from action detection models. During the third round of transmission, units related to style and adjectives, which share similar characteristics, are predominantly selected. This indicates that the execution of

perceptual extraction models, such as those used for sentiment analysis and style detection, can be appropriately delayed. Units of other types are typically chosen for transmission at later rounds due to their lesser contribution to the semantic information of the inferred images. Additionally, the results indicate that the obtained RL-based TPE approach terminates the extraction process early and discards the transmission of a certain number of text units with a probability of 7.3%. We present the components of the discarded text units in Fig. 6 (b), which shows that the majority of discarded units fall into the ‘OTHERS’ category, such as ‘of’, ‘a’, and ‘the’. This indicates that in the current inference task, these units represent semantic information that is less relevant to the task. Finally, we analyze the number of text units transmitted at different time intervals using the TPE method, as presented in Fig. 6 (c). The results indicate that a large amount of text units are transmitted during the earlier transmission. This is primarily because the semantic guidance effect is most effective at the initial stage of denoising. Consequently, the system prioritizes maintaining a high-performance score, even at the expense of some latency. In the subsequent transmission rounds, the number of transmitted text units decreases to approximately two. During these phases, the extraction latency and segmented denoising duration are closely aligned, indicating the effective parallelization of these processes. In the final transmission rounds, the number of transmitted text units significantly decreases. This reduction is primarily attributed to the smaller number of long prompts in the dataset and the discarding phenomenon of the TPE method.

3) *Visual Demonstration and Comparison of Denoising Processes*: In Fig. 7, we present a visual demonstration of the denoising processes of the conventional GSC, PGSC, and the TPE-assisted PGSC (TPE-PGSC) approaches. In the conventional GSC framework, the semantic extraction and inference processes are separated. Therefore, the diffusion model can condition on the complete prompt throughout the inference process, as shown in Fig. 7 (a). Although this traditional architecture ensures the quality of inferred images, it also introduces significant latency. In the PGSC framework, although the parallel execution of the semantic extraction and inference processes significantly reduces delays, the quality of the inferred images cannot be guaranteed. As depicted in Fig. 7

<sup>5</sup>Note that to eliminate the impact of different proportions of text unit types in the dataset on the results, we compute the statistics based on their respective proportions over the time series. Consequently, the sum of their proportions at any given moment may exceed 100%.

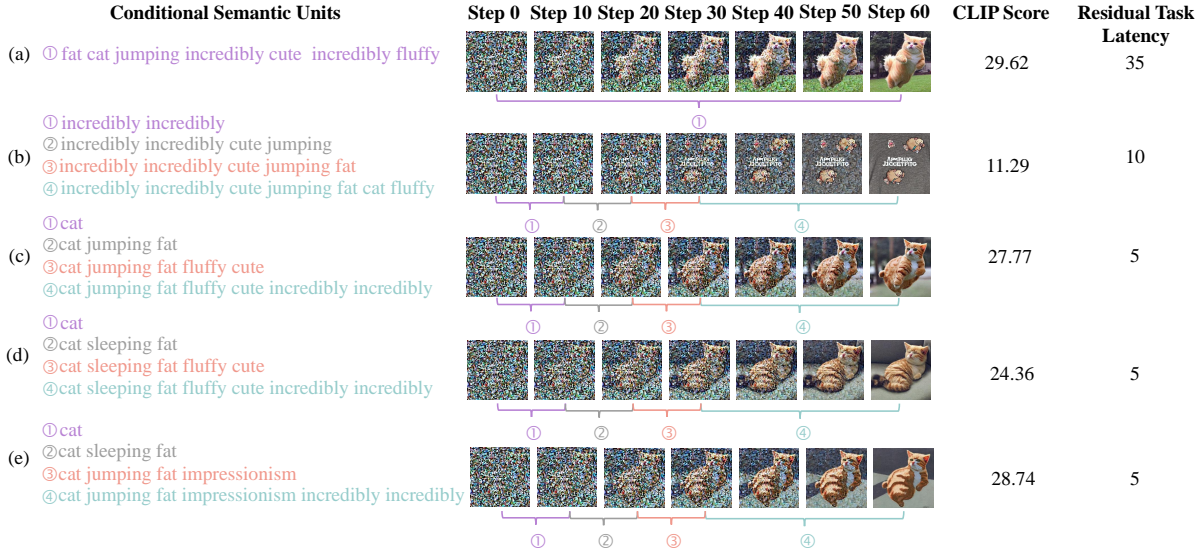


Fig. 7. Visual demonstration and comparison of denoising processes: (a) Conventional GSC, conditioned on the entire prompt throughout the inference process; (b) PGSC, conditioned on text units received in a random sequence over time; (c) TPE-PGSC, conditioned on text units received in a sequence guided by TPE; (d) TPE-PGSC, with changes in an action-related text unit; (e) TPE-PGSC, incorporating a specific style. The residual task latency is defined as the portion of task latency that extends beyond the fixed inference duration and measured in denoising steps.

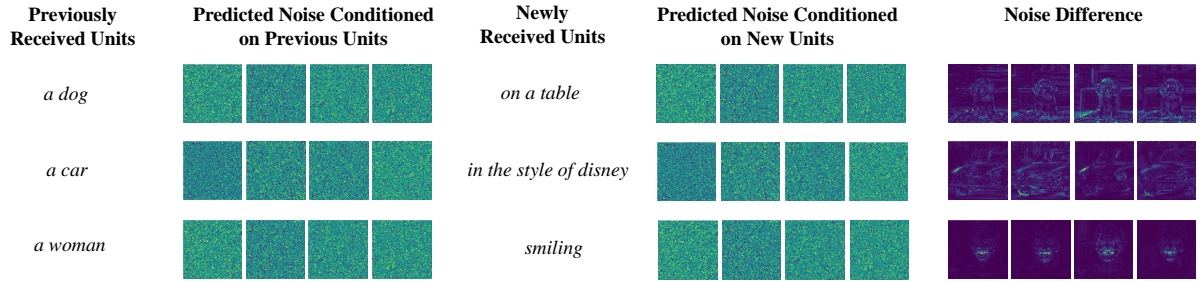


Fig. 8. Detailed visual demonstration of the semantic difference calculation module’s working process. To elucidate the information captured by each feature map, we unfold the conditional noise predictions along the second dimension and visualize the four  $64 * 64$  matrices individually.

(b), the arbitrary assignment of semantic extraction sequences may substantially compromise the quality of inference. In Fig. 7 (c)-(e), we present the denoising processes in the TPE-PGSC framework. By applying lessons learned from RL, we carefully control the sequence in which different categories of semantic units are transmitted, thereby achieving varied degrees of control over the denoising process at different noise levels. This approach ensures that the final inferred image more closely aligns with the original prompt.

### B. Effectiveness of Sequential Conditional Denoising

In this section, we evaluate the performance of the sequential conditional denoising (SCD) method. Initially, we present visual demonstrations of the inputs and outputs from the proposed semantic difference calculation module, showcasing how this module precisely amplifies the modifications required for newly received text units. Subsequently, we provide a visual analysis of the impact of the intervention factor  $\alpha$  on the method’s performance.

1) *Visual Demonstration of the Working Process of Semantic Difference Calculation Module:* A visual representation of the working processes of the semantic difference calculation module is depicted in Fig. 8. We segment each prompt into two sets, displayed in the first and second columns, respectively. Initially, we transmit the units from the first column to the receiver to initiate the image inference process. Subsequently, after a 20-step denoising period, we transmit the units from the second column. As shown in Fig. 8, direct observation of the predicted noise conditioned on both the previous and the new units may not provide useful information; however, the differences between them reveal significant semantic meanings. This distinction presents the necessary adjustments in the noise space to effectively incorporate the influence of late-arrived units on the inference results. Specifically, in the first transmission scenario, depicted in the first row, the noise difference highlights the edge of the table and the dog’s foot. In the second transmission scenario, the edge of the car, particularly the headlights and tires, is emphasized. This emphasis is attributed to the distinctive, rounded contours

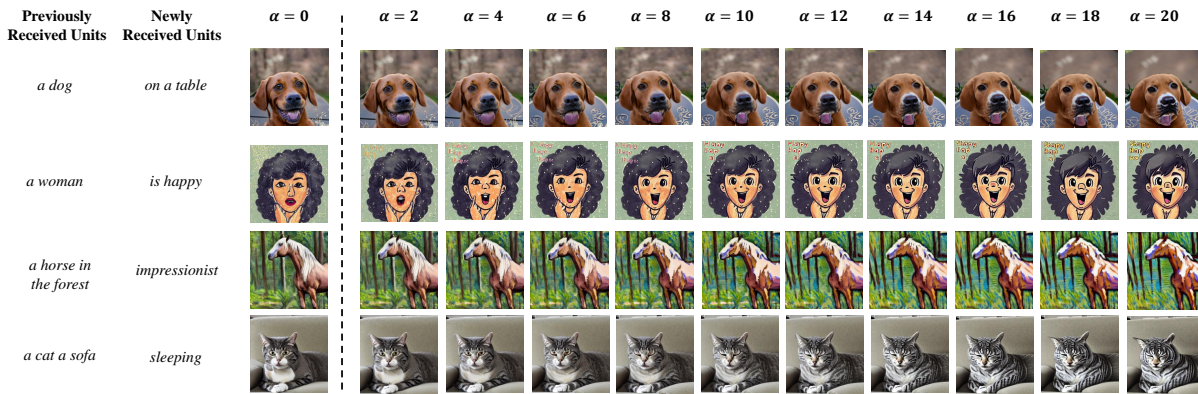


Fig. 9. Visual illustrations of changes in intervention factor values on the inferred images.

characteristic of objects depicted in the Disney style. In the third transmission scenario, the bright areas in the noise difference image represent the woman’s mouth, which is the focal point for achieving the ‘smiling’ directive. By employing this module, we can precisely identify the portions of the noise space that the newly arrived semantic features aim to modify.

2) *Visual Demonstration of Various Intervention Values on the Inferred Images:* In Fig. 9, we examine the influence of the intervention factor  $\alpha$  specified in Equation (14) on the images inferred under different scenarios involving the transmission of various types of semantic units. Similarly, the units from the first column are transmitted to the receiver to commence the image generation process. Following a 20-step denoising period, the units from the second column are subsequently transmitted. We compare the sequential conditional denoising results with intervention factors ranging from 2 to 20 against some representative inference failures of the PGSC, which are depicted in the column marked  $\alpha = 0$ . Specifically, in the transmission scenario shown in the first row, when  $\alpha = 0$ , the inferred image resembles an outdoor scene, with wild grass on either side of the dog and the object beneath the dog appearing more like wooden steps. With the increase of  $\alpha$ , the extended wooden steps transform into a round, enclosed table, and a chair commonly associated with the table appears in the background. Even the wild grass on either side of the dog gradually turns into patterns on the table. In the transmission scenario described in the second row, the image corresponding to  $\alpha = 0$  depicts the woman with an expression that is more serious than happy. With the increase of  $\alpha$ , we observe that the woman’s mouth opens wider due to smiling, and her eyes gradually become rounder, displaying an increasingly happy trend. Significantly, starting from  $\alpha = 10$ , we begin to observe the emergence of laugh lines and nasolabial folds on the woman’s face, attributable to the contraction of facial muscles during smiling. In the third row, we investigate the image inference scenario involved with style indications. Although style-related prompts demonstrate greater robustness to the position of the inserted timestamp relative to the total timestamp, from the perspective of color and line contrast, an enhancement in style with the increase of  $\alpha$  is still observable. In this last row, we demonstrate the enhancements our proposed method brings to action-related

units received later. When  $\alpha = 0$ , the cat’s eyes in the image are wide open, exhibiting no signs of sleepiness. However, as  $\alpha$  increases from 2 to 6, the cat’s eyes progressively close. At  $\alpha = 8$ , the cat’s open eyes and its facial patterns begin to blend together. From  $\alpha = 10$  onward, the cat’s eyes are clearly closed, with the area previously occupied by the eyes now resembling the pattern of eyelids. Notably, at  $\alpha = 18$  and  $\alpha = 20$ , the cat’s ears are observed to droop, indicative of drowsiness. However, it is important to note that these visual results also demonstrate that a higher  $\alpha$  is not always better. We observe that when  $\alpha$  is very high, the semantic information related to previously received units is diminished in the inferred images. For example, at  $\alpha = 20$ , a strange pattern appears on the dog’s nose in the first column, and the aesthetics of the woman’s image in the second column are also reduced. Therefore, in practice, it is necessary to design an appropriate intervention value to balance the influence of previously received units and newly received units on the final inferred image.

### C. Overall Analysis of Combined Refinements

In this section, we investigate whether the TPE and SCD methods can work together to enhance the system performance of the PGSC framework. Initially, we explore the impact of various intervention factors of the SCD method to find a more suitable one for use with the TPE method under different extraction latency settings. Following this, we synergistically integrate these enhancements into the PGSC framework, ultimately establishing the FAST-GSC framework. Subsequently, we present numerical results, comparing the conventional GSC framework with the PGSC framework featuring different enhancements, and the FAST-GSC framework.

1) *Numerical Results of Various Intervention Factor Values on the System Performance:* Herein, we examine the variations in CLIP scores with respect to the intervention factor  $\alpha$ , aiming to identify a more suitable value to work with TPE methods under our default and two alternative extraction latency settings. To synchronize with the training process of the TPE method, we segment every 5 denoising steps for the alternative setting where the latency for extracting a single semantic unit  $\tau_e$  equals the duration of 2.5 denoising steps,



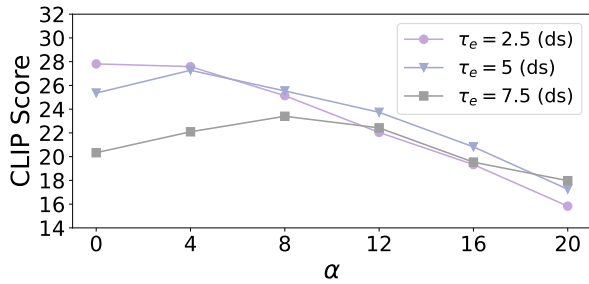


Fig. 10. Variations in CLIP scores relative to the intervention factor under different latencies for extracting a single semantic unit, with extraction latency measured in denoising steps (ds).

every 10 denoising steps for the default setting where the latency for extracting a single semantic unit  $\tau_e$  equals the duration of 5 denoising steps, and every 15 denoising steps for the alternative setting where the latency for extracting a single semantic unit  $\tau_e$  equals the duration of 7.5 denoising steps. As illustrated in Fig. 10, under the same denoising speed, a higher intervention value is desired for systems with longer extraction latency. This is due to the fact that, once the initial semantic units initiate the denoising process, the extended extraction latency prolongs the incorporation time for each subsequent semantic unit. Consequently, the residual noise level in intermediate results is lower compared to settings with shorter extraction latency. In such scenarios, a greater noise space intervention capability is necessary to adjust the noise space effectively and incorporate the newly arrived units under conditions of extended extraction latency.

## 2) Numerical Results of Task Performance and Latency:

Herein, we focus on our default extraction speed setting, where the extraction latency for distilling one text unit from the source image corresponds to 5 denoising steps. Based on the numerical results assessing the impact of various intervention factor values on system performance, we set the intervention factor  $\alpha$  at 4 to synergistically integrate the TPE and SCD methods to establish the FAST-GSC framework. Finally, we present the task performance, latency count and task efficiency results of the conventional GSC, PGSC with random transmission order, TPE-PGSC, SCD-PGSC, and FAST-GSC in Fig. 11. Herein, task efficiency is defined as the ratio of task performance to residual task latency. Numerical results indicate that, although the direct implementation of PGSC effectively reduces system latency, it leads to significant performance degradation. Enhanced by the TPE method, the TPE-PGSC framework further reduces the residual task latency of PGSC by 21% and boosts the CLIP score by 26%. Additionally, the SCD-PGSC framework improves the CLIP score by 8% over the direct PGSC implementation. In terms of task efficiency, the FAST-GSC framework emerges as the most beneficial. It achieves a performance score comparable to the conventional GSC architecture while realizing a 52% reduction in residual task latency.

## VI. CONCLUSION

In this paper, we have proposed a fast and adaptive semantic transmission design to reduce task latency within the conventional GSC framework while maintaining high task performance. Specifically, to decrease task latency, we have designed a communication mechanism that incorporates parallel semantic extraction and inference. Based on the direct implementations of the proposed mechanism, we have observed that the sequential dependencies among various semantic units and the reception immediacy of individual units significantly influence its task performance. Given that, we have implemented a RL-guided temporal prompt engineering method at the transmitter to sequence the extraction models according to their semantic sequential dependencies. Furthermore, we have mitigated the stringent reception immediacy by proposing a sequential conditional denoising approach based on a semantic difference calculation module at the receiver. Simulation results have validated the effectiveness of our proposed framework and demonstrated its significant potential for maintaining high task performance while reducing task latency.

Looking to the future, our devised framework can be extended to multi-user communication scenarios. By segmenting large semantic information blocks into smaller units, we enable more fine-grained semantic importance analysis and adaptive transmission design according to the users' diverse task requirements. This approach also reduces the data delivered to a user at any given time, thereby mitigating network congestion in multi-user communication networks. Besides, our framework can also be utilized to enhance the communication efficiency for multi-modal data transmission. Specifically, it can be adapted to dynamically determine the transmission priority and resource allocation for different types of data, such as text, images, and video, based on their semantic significance and the current network conditions. Such directions are critical for the development of GSC and are worth further research.

## REFERENCES

- [1] W. Yang, Z. Xiong, Y. Yuan, W. Jiang, T. Q. S. Quek, and M. Debbah, "Agent-driven generative semantic communication for remote surveillance," arXiv preprint arXiv:2404.06997, 2024.
- [2] Y. Wang, W. Yang, Z. Xiong, Y. Zhao, T. Q. S. Quek, and Z. Han, "Harnessing the power of AI-generated content for semantic communication," *IEEE Network*, 2024, to appear.
- [3] L. Xia, Y. Sun, C. Liang, L. Zhang, M. A. Imran, and D. Niyato, "Generative AI for semantic communication: Architecture, challenges, and outlook," arXiv preprint arXiv:2308.15483, 2024.
- [4] W. Yang, Z. Xiong, Y. Yuan, and T. Q. Quek, "Semantic change driven generative semantic communication framework," arXiv preprint arXiv:2309.12775, 2023.
- [5] J. Wang, H. Du, D. Niyato, J. Kang, Z. Xiong, D. Rajan, S. Mao, and X. Shen, "A unified framework for guiding generative AI with wireless perception in resource constrained mobile edge networks," *IEEE Transactions on Mobile Computing*, 2024, to appear.
- [6] R. Zhang, K. Xiong, H. Du, D. Niyato, J. Kang, X. Shen, and H. V. Poor, "Generative AI-enabled vehicular networks: Fundamentals, framework, and case study," arXiv preprint arXiv:2304.11098, 2023.
- [7] H. Chen, F. Fang, and X. Wang, "Semantic extraction model selection for IoT devices in edge-assisted semantic communications," *IEEE Communications Letters*, 2024.
- [8] J. Ho, A. Jain, and P. Abbeel, "Denoising diffusion probabilistic models," *Advances in Neural Information Processing Systems*, vol. 33, pp. 6840–6851, 2020.

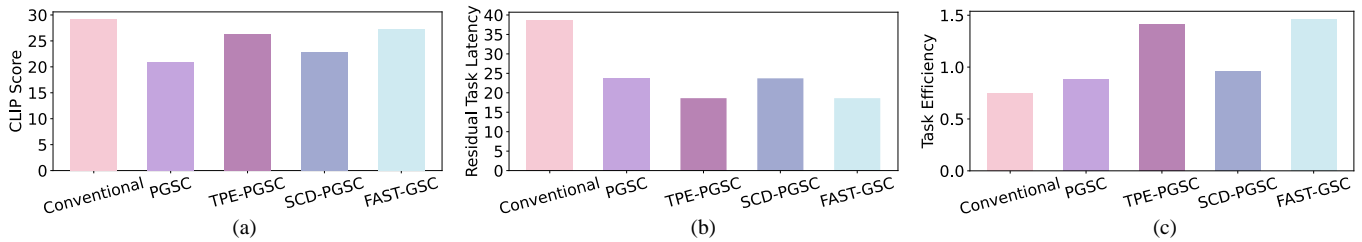


Fig. 11. Numerical results: (a) Task performance, measured by CLIP score; (b) Residual task latency, defined as the portion of task latency that extends beyond the fixed inference duration and measured in denoising steps; (c) Task efficiency, defined as the ratio of the task performance to the latency count.

[9] O. Avrahami, D. Lischinski, and O. Fried, “Blended diffusion for text-driven editing of natural images,” in *Proceedings of the IEEE/CVF Conference on Computer Vision and Pattern Recognition*, 2022, pp. 18 208–18 218.

[10] R. Huang, J. Huang, D. Yang, Y. Ren, L. Liu, M. Li, Z. Ye, J. Liu, X. Yin, and Z. Zhao, “Make-an-audio: Text-to-audio generation with prompt-enhanced diffusion models,” in *Proceedings of the International Conference on Machine Learning*, 2023, pp. 13 916–13 932.

[11] T. Amit, T. Shaharbandy, E. Nachmani, and L. Wolf, “Segdiff: Image segmentation with diffusion probabilistic models,” arXiv preprint arXiv:2112.00390, 2021.

[12] Y. Li, H. Liu, Q. Wu, F. Mu, J. Yang, J. Gao, C. Li, and Y. J. Lee, “Gligen: Open-set grounded text-to-image generation,” in *Proceedings of the IEEE/CVF Conference on Computer Vision and Pattern Recognition*, 2023, pp. 22 511–22 521.

[13] G. Zheng, X. Zhou, X. Li, Z. Qi, Y. Shan, and X. Li, “Layoutdiffusion: Controllable diffusion model for layout-to-image generation,” in *Proceedings of the IEEE/CVF Conference on Computer Vision and Pattern Recognition*, 2023, pp. 22 490–22 499.

[14] H. Du, R. Zhang, D. Niyato, J. Kang, Z. Xiong, D. I. Kim, X. Shen, and H. V. Poor, “Exploring collaborative distributed diffusion-based ai-generated content (AIGC) in wireless networks,” *IEEE Network*, vol. 38, no. 3, pp. 178–186, 2024.

[15] H. Du, R. Zhang, D. Niyato, J. Kang, Z. Xiong, S. Cui, X. Shen, and D. I. Kim, “User-centric interactive AI for distributed diffusion model-based AI-generated content,” arXiv preprint arXiv:2311.11094, 2023.

[16] G. Xie, Z. Xiong, X. Zhang, R. Xie, S. Guo, M. Guizani, and H. V. Poor, “GAI-IoV: Bridging generative ai and vehicular networks for ubiquitous edge intelligence,” *IEEE Transactions on Wireless Communications*, 2024, to appear.

[17] Z. Shi, X. Zhou, X. Qiu, and X. Zhu, “Improving image captioning with better use of captions,” arXiv preprint arXiv:2006.11807, 2020.

[18] R. Rombach, A. Blattmann, D. Lorenz, P. Esser, and B. Ommer, “High-resolution image synthesis with latent diffusion models,” in *Proceedings of the IEEE/CVF Conference on Computer Vision and Pattern Recognition*, New Orleans, LA, USA, Jun. 2022, pp. 10 684–10 695.

[19] J. Achiam *et al.*, “GPT-4 technical report,” arXiv preprint arXiv:2303.08774, 2023.

[20] T. Brown *et al.*, “Language models are few-shot learners,” *Advances in Neural Information Processing Systems*, vol. 33, pp. 1877–1901, 2020.

[21] T. Gao, A. Fisch, and D. Chen, “Making pre-trained language models better few-shot learners,” in *Proceedings of the 59th Annual Meeting of the Association for Computational Linguistics and the 11th International Joint Conference on Natural Language Processing (Volume 1: Long Papers)*, Aug. 2021, pp. 3816–3830.

[22] Y. Liu, H. Du, D. Niyato, J. Kang, S. Cui, X. Shen, and P. Zhang, “Optimizing mobile-edge AI-generated everything (AIGX) services by prompt engineering: Fundamental, framework, and case study,” *IEEE Network*, 2024, to appear.

[23] Y. Feng, X. Wang, K. K. Wong, S. Wang, Y. Lu, M. Zhu, B. Wang, and W. Chen, “PromptMagician: Interactive prompt engineering for text-to-image creation,” *IEEE Transactions on Visualization and Computer Graphics*, vol. 30, no. 1, pp. 295–305, 2024.

[24] H. Cai, L. Zhu, and S. Han, “Proxylessnas: Direct neural architecture search on target task and hardware,” arXiv preprint arXiv:1812.00332, 2018.

[25] S. Han, H. Mao, and W. J. Dally, “Deep compression: Compressing deep neural networks with pruning, trained quantization and Huffman coding,” arXiv preprint arXiv:1510.00149, 2015.

[26] G. Hinton, O. Vinyals, and J. Dean, “Distilling the knowledge in a neural network,” arXiv preprint arXiv:1503.02531, 2015.

[27] T. Ghandi, H. Pourreza, and H. Mahyar, “Deep learning approaches on image captioning: A review,” *ACM Computing Surveys*, vol. 56, no. 3, pp. 1–39, 2023.

[28] A. Zur, E. Kreiss, K. D’Oosterlinck, C. Potts, and A. Geiger, “Updating clip to prefer descriptions over captions,” arXiv preprint arXiv:2406.09458, 2024.

[29] J. Ho and T. Salimans, “Classifier-free diffusion guidance,” arXiv preprint arXiv:2207.12598, 2022.

[30] J. Song, C. Meng, and S. Ermon, “Denoising diffusion implicit models,” arXiv preprint arXiv:2010.02502, 2020.

[31] G. Jocher, A. Chaurasia, and J. Qiu, “YOLO by Ultralytics,” Jan. 2023. [Online]. Available: <https://github.com/ultralytics/ultralytics>

[32] K. Dan, Y. Liangzhe, and L. Khanh, “Video Classification on Edge Devices with TensorFlow Lite and MoViNet,” Apr. 2022. [Online]. Available: <https://blog.tensorflow.org/2022/04/video-classification-on-edge-devices.html>

[33] K. Chen *et al.*, “MMDetection: Open mmlab detection toolbox and benchmark,” arXiv preprint arXiv:1906.07155, 2019.

[34] A. Jon, “Stable Diffusion LoRA Training – Consumer GPU Analysis,” Dec. 2023. [Online]. Available: <https://www.pugetsystems.com/labs/articles/stable-diffusion-lora-training-consumer-gpu-analysis/>

[35] X. Liu, X. Zhang, J. Ma, J. Peng *et al.*, “Instaflow: One step is enough for high-quality diffusion-based text-to-image generation,” in *Proceedings of the Twelfth International Conference on Learning Representations*, 2023.

[36] F. Ian, “Benchmarking the Global 5G Experience — June 2023,” Jun. 2023. [Online]. Available: <https://www.opensignal.com/2023/06/30/benchmarking-the-global-5g-experience-june-2023>

[37] J. Hessel, A. Holtzman, M. Forbes, R. L. Bras, and Y. Choi, “Clipscore: A reference-free evaluation metric for image captioning,” arXiv preprint arXiv:2104.08718, 2021.

[38] A. Radford *et al.*, “Learning transferable visual models from natural language supervision,” in *Proceedings of the International Conference on Machine Learning*. PMLR, 2021, pp. 8748–8763.

[39] K. Lu, R. Li, X. Chen, Z. Zhao, and H. Zhang, “Reinforcement learning-powered semantic communication via semantic similarity,” arXiv preprint arXiv:2108.12121, 2021.

[40] D. Bahdanau, P. Brakel, K. Xu, A. Goyal, R. Lowe, J. Pineau, A. Courville, and Y. Bengio, “An actor-critic algorithm for sequence prediction,” arXiv preprint arXiv:1607.07086, 2016.

[41] J. Schulman, F. Wolski, P. Dhariwal, A. Radford, and O. Klimov, “Proximal policy optimization algorithms,” arXiv preprint arXiv:1707.06347, 2017.

[42] S. Huang and S. Ontañón, “A closer look at invalid action masking in policy gradient algorithms,” arXiv preprint arXiv:2006.14171, 2020.

[43] Z. J. Wang, E. Montoya, D. Munechika, H. Yang, B. Hoover, and D. H. Chau, “Diffusiondb: A large-scale prompt gallery dataset for text-to-image generative models,” arXiv preprint arXiv:2210.14896, 2022.

[44] V. Liu and L. B. Chilton, “Design guidelines for prompt engineering text-to-image generative models,” in *Proceedings of the 2022 CHI Conference on Human Factors in Computing Systems*, 2022, pp. 1–23.

[45] M. Honnibal, I. Montani, S. Van Landeghem, and A. Boyd, “spaCy: Industrial-strength Natural Language Processing in Python,” 2020.

[46] Y. Liu, H. Du, D. Niyato, J. Kang, Z. Xiong, S. Mao, P. Zhang, and X. Shen, “Cross-modal generative semantic communications for mobile aigc: Joint semantic encoding and prompt engineering,” arXiv preprint arXiv:2404.13898, 2024.